Archival Report

Biological Psychiatry

Oscillatory Neural Signatures of Visual Perception Across Developmental Stages in Individuals With 22q11.2 Deletion Syndrome

Valentina Mancini, Vincent Rochas, Martin Seeber, Tineke Grent-'t-Jong, Tonia A. Rihs, Caren Latrèche, Peter J. Uhlhaas, Christoph M. Michel, and Stephan Eliez

ABSTRACT

BACKGROUND: Numerous behavioral studies have highlighted the contribution of visual perceptual deficits to the nonverbal cognitive profile of individuals with 22q11.2 deletion syndrome. However, the neurobiological processes underlying these widespread behavioral alterations are yet to be fully understood. Thus, in this paper, we investigated the role of neural oscillations toward visuoperceptual deficits to elucidate the neurobiology of sensory impairments in deletion carriers.

METHODS: We acquired 125 high-density electroencephalography recordings during a visual grating task in a group of 62 deletion carriers and 63 control subjects. Stimulus-elicited oscillatory responses were analyzed with 1) time-frequency analysis using wavelets decomposition at sensor and source level, 2) intertrial phase coherence, and 3) Granger causality connectivity in source space. Additional analyses examined the development of neural oscillations across age bins.

RESULTS: Deletion carriers had decreased theta-band (4–8 Hz) and gamma-band (58–68 Hz) spectral power compared with control subjects in response to the visual stimuli, with an absence of age-related increase of theta- and gamma-band responses. Moreover, adult deletion carriers had decreased gamma- and theta-band responses but increased alpha/beta desynchronization (10–25 Hz) that correlated with behavioral performance. Granger causality estimates reflected an increased frontal-occipital connectivity in the beta range (22–40 Hz).

CONCLUSIONS: Deletion carriers exhibited decreased theta- and gamma-band responses to visual stimuli, while alpha/beta desynchronization was preserved. Overall, the lack of age-related changes in deletion carriers implicates developmental impairments in circuit mechanisms underlying neural oscillations. The dissociation between the maturation of theta/gamma- and alpha/beta-band responses may indicate a selective impairment in supragranular cortical layers, leading to compensatory top-down connectivity.

https://doi.org/10.1016/j.biopsych.2022.02.961

Prominent disruptions of brain oscillations, particularly in the gamma-band range, have been observed in patients with schizophrenia and during earlier stages of the disease in patients with a first episode of psychosis and individuals at clinical high risk for psychosis (1–4). The majority of the studies have shown impaired gamma-band response to auditory stimuli (2), while it has been suggested that abnormalities in high-frequency brain oscillations might extend to other sensory modalities. In particular, reduced power and synchronization of gamma-band oscillations during visual processing have been shown (1,2,5–10), which is consistent with psychophysical data in patients with schizophrenia (11). Moreover, visual gamma-band impairments have been observed already at the first episode of psychosis stage (12). However, it remains to be elucidated whether such impairment predates the emergence of clinically detectable psychotic symptoms.

Gamma-band oscillations have been causally related to the activity of fast-spiking parvalbumin interneurons (13–17), which undergo profound maturational changes during the transition from adolescence to adulthood (18,19), including epigenetic modifications (20,21), and fluctuations in the glutamatergic drive onto parvalbumin interneurons through NMDA receptors (22,23). There is also evidence for late maturation of gamma-band oscillations in human electroencephalography (EEG) data (24). Studies on preclinical models of schizophrenia have further demonstrated that schizophrenia-like deficits, including gamma-band dysfunction, appear in early adulthood and can be rescued during a sensitive time window in late adolescence (25).

Genetic models of schizophrenia, such as the 22q11.2 deletion syndrome (22q11DS), are ideally suited to prospectively study neurodevelopmental changes associated with psychosis risk (26). Indeed, 22q11.2 deletion carriers are characterized by a high proneness to develop psychiatric disorders, in particular psychosis, with an estimated lifetime prevalence of around 30% (27,28). Behavioral, neuroimaging,

SEE COMMENTARY ON PAGE 338

ISSN: 0006-3223

Biological Psychiatry September 1, 2022; 92:407–418 www.sobp.org/journal

and genetic findings highlighted a shared neurobiological vulnerability between 22q11DS and idiopathic psychosis (29–31). For instance, 22q11DS is characterized by impaired visuospatial processing (32) that encompasses deficits in the discrimination of local details and selective deficits in visuospatial memory (32–35), which could reflect findings of reduced activation in ventral and dorsal streams (36,37). Consistently, studies in mice with the homologous deletion were characterized by deficits in gamma- and theta-band oscillations in V1 (38).

Risk genes such as *DGCR8*, *PRODH*, *CXCR4*, and *ZDHHC8* have been implicated in axonal growth and glutamatergic and GABAergic (gamma-aminobutyric acidergic) neural transmission (39–43), which are important for the generation of gamma-band oscillations (15). In line with this evidence, previous studies in human deletion carriers have identified deficient gamma-band response during auditory processing (44,45), but the ability of visual cortices to generate neural oscillations has not been investigated so far.

This study investigated oscillatory responses during visual perception and their relationship with brain development in deletion carriers to address this important question. Visual perception results from the interplay between neuronal oscillations at distinct frequency bands, with gamma- and theta-band oscillations subserving perceptual information transfer in low-level regions, while top-down beta-band oscillations convey feedback signaling according to the behavioral context (46,47). Moreover, studies have shown that supragranular layers predominantly propagate feedforward information in the gamma-band frequency, while infragranular layers subserve feedback activity in the beta-band frequency (46–48). For this reason, we additionally estimated Granger causality (GC) connectivity between high- and low-order areas in the visual system in source-reconstructed EEG data.

We expected to find a selective deficit in stimulus-induced gamma- and theta-band responses (25) and a lack of age-related increase in gamma-band power with respect to the control group as supported by studies in the homologous mouse model of 22q11DS (25). Furthermore, we hypothesized that deletion carriers would express increased top-down connectivity as a compensatory mechanism for deficits in visual circuits. Finally, we conducted exploratory analyses to test the association between oscillatory response and the degree of psychotic symptoms in deletion carriers.

METHODS AND MATERIALS

Recruitment and Assessment of Patients

Individuals with 22q11DS and control subjects were recruited in the context of the 22q11DS Swiss Cohort (details available in the Supplement).

The occurrence of attenuated psychotic symptoms (APSs) was assessed in deletion carriers by means of the Structured Interview for Psychosis-Risk Syndromes (49). Deletion carriers were divided into subgroups according to the presence of moderate to severe APS symptoms, using a cut-off score of 3 or higher in at least one of the corresponding items for positive symptoms of the Structured Interview for Psychosis-Risk Syndromes.

Participants

Of 145 potential participants (age range = 7–30 years), 6 deletion carriers were not included in the study because of a medical history of epilepsy or epileptic seizures. Fourteen datasets (8 deletion carriers and 6 control subjects) were additionally excluded from the analyses because the number of accepted clean epochs with a correct answer was $n < 40$, resulting in 63 subjects with 22q11DS (mean age = 17.3 ± 6 years, 26 female) and 62 control subjects (mean age = 17.2 ± 7 years, 24 female). The participants of each group were divided into age bins: childhood (from 7 to 13 years; $n = 39$), adolescence (from 14 to 18 years; $n = 39$), and adulthood (≥19 years; $n = 47$) for the age-related analyses. Control subjects and deletion carriers were overall age and sex matched, as for age subgroups (Table 1).

Visual Paradigm

The visual paradigm consisted of a centrally presented, circular sine wave grating (Figure 1). The circular grating drifted inward toward the fixation point position, and the speed of this contraction increased (velocity step at 2.2 deg/s) at a randomized time point between 750 and 3000 ms after stimulus onset (12,50). The experimental protocol comprised 240 trials divided into three runs of 80 trials. Participants were instructed to press a button as soon as they noticed a speed increase. Stimulus offset was followed by a period of 1000 ms during which subjects were given visual feedback depending on their response. Before beginning the experiment, all participants underwent a training session with one researcher to be sure that they understood the task. Behavioral measures were calculated as the percentage of correct answers of the 240 trials and average reaction time.

EEG Data Acquisition During Visual Paradigm and Preprocessing

EEG data were continuously recorded with a sampling rate of 1000 Hz using a 256-electrode Hydrocel cap (Magstim-EGI) referenced to the vertex (Cz). The impedance was kept below 30 kΩ for all electrodes and below 10 kΩ for the reference and ground electrodes.

The preprocessing steps, including bandpass filtering, exclusion of artifactual periods, interpolation of noisy channels, and re-referencing (51–53) were performed using the free academic software Cartool (45,54). For further details, see the Supplement.

EEG Time-Frequency and Intertrial Phase Coherence Analyses

Only epochs with correct behavioral responses were considered for EEG analysis. Owing to the imbalance between the number of correct responses between groups, a percentage of the total epochs based on the distribution of the entire sample was randomly selected in control subjects to have a comparable number of epochs (control subjects: 129.2 ± 33.4; 22q11DS: 120.9 ± 49.5).

Time-frequency analysis was performed using Morlet transform (frequencies from 2 to 120 Hz, centered on steps of 2 Hz, with adapted resolution according to the full width at half maximum scheme) in MATLAB (version 2018b; The

Table 1. Demographic Information and Medical History Comprising Psychiatric Disorders According to DSM-5 and Medications Usage in Control Subjects and Deletion Carriers and in the Subgroups of Deletion Carriers Older Than 14 Years With and Without Psychotic Symptoms

Demographic and Clinical Information	Control Subjects	Deletion Carriers	*p* Value	Nonpsychotic	Psychotic	*p* Value
Number of Subjects (% F)	62 (50%)	63 (49.2%)	.76	28 (71.4%)	12 (58.3%)	.27
Age, Years, Mean ± SD	17.3 ± 6.1	17.2 ± 7	.93	21.6 ± 5.7	20.9 ± 6.1	.78
Age Range, Years	7–30	7–30	N/A	14–30	14–30	N/A
FSIQ, Mean ± SD	110.1 ± 17	75 ± 12.6	<.01	73.3 ± 10.5	70.7 ± 16.4	.53
Behavioral Performance, Number of Correct Answers, Mean ± SD	158.3 ± 34.8	206.4 ± 29.9	<.01	167.8 ± 26.7	167 ± 24.9	.93
Children, *n* (Mean Age ± SD), % F	16 (10.2 ± 2.4), 50%	23 (10.4 ± 1.5), 47.8%	.76	N/A	N/A	N/A
Adolescents, *n* (Mean Age ± SD), % F	23 (15.7 ± 1.4), 47.8%	16 (15.4 ± 1.3), 43.8%	.4	N/A	N/A	N/A
Adults, *n* (Mean Age ± SD), % F	23 (23.5 ± 3.3), 52.2%	24 (25.4 ± 3.8), 54.2%	.14	N/A	N/A	N/A
Subjects Medicated, *n* (%)	0	24 (38.1%)	N/A	10 (35.7%)	7 (58.3%)	.18
Psychostimulants	0	15 (23.8%)	N/A	7 (25%)	3 (25%)	.95
Antidepressants	0	12 (19%)	N/A	7 (25%)	5 (41.7%)	.29
Antipsychotics	0	10 (15.9%)	N/A	0 (0%)	7 (58.3%)	<.01
Subjects Meeting Criteria for Psychiatric Diagnosis, *n* (%)	0	41 (65.1%)	N/A	14 (50%)	8 (66.7%)	.33
ADHD	0	32 (50.8%)	N/A	11 (39.3%)	6 (50%)	.81
Anxiety disorders	0	30 (47.6%)	N/A	10 (35.7%)	7 (58.3%)	.34
Mood disorders	0	4 (6.3%)	N/A	2 (7.1%)	2 (16.7%)	.50
Psychosis spectrum disorders	0	13 (20.6%)	N/A	0	3 (25%)	<.01
SIPS Positive Symptoms Score, Mean ± SD	N/A	0.8 ± 1	N/A	0.3 ± 0.4	2.1 ± 1.2	<.01
SIPS Negative Symptoms Score, Mean ± SD	N/A	2.1 ± 0.9	N/A	2 ± 0.7	2.9 ± 0.9	.01

p Values refer to the comparison between groups and subgroups performed with two-tailed *t* test and χ^2 test when appropriate.
ADHD, attention-deficit/hyperactivity disorder; F, female; FSIQ, Full Scale IQ; N/A, not applicable; SIPS, Structured Interview for Psychosis-Risk Syndromes.

MathWorks, Inc.). Time epochs from −1.5 to +1.5 seconds relative to the stimulus onset were averaged to event-related spectral perturbations (ERSPs) and normalized by the baseline period (−1.5 to −0.3 seconds) (55). Intertrial phase coherence (ITPC) amplitudes were also calculated from Morlet transform (56). At the sensor level, a cluster of predefined occipitoparietal electrodes was considered for further analyses. To investigate the interaction of spectral response with behavioral and clinical variables, neurophysiological indices were also calculated from averages of the ERSP along frequency bands of interest for theta, alpha/beta, and gamma and in time from 0.25 to 0.75 seconds for gamma and alpha/beta and from 0 to 0.4 seconds for theta.

For source analysis, the inverse solution (IS) was computed using Cartool version 61 based on individual T1-weighted images preprocessed in FreeSurfer image analysis suite, version 6.0 (57). An approximate number of 5000 solution points were distributed in the individually segmented gray matter mask. We used the Locally Spherical Model with Anatomical Constraints method for the lead field computation, which was age adjusted to reflect differences across age in skull conductivity and thickness (58,59). A distributed linear IS (Local AutoRegressive Average) was used to compute a transformation matrix from sensor level to IS (58). We obtained an individual Desikan-Killiany parcellation (60) from FreeSurfer. This individual parcellation natively aligned on the brain of each individual was then used to label the 5000 solution points from the IS model in 84 regions of interest (ROIs) covering cortical and subcortical structures. Using this individual IS model, time-frequency decomposition data from the surface were projected to the source space level and gathered in ROIs representing the whole brain.

GC Analysis

GC functional connectivity was computed in source space with a nonparametric approach (61) implemented in the MATLAB Toolbox FieldTrip (62). First, preprocessed EEG data were transformed to the singular value decomposition of the signal for each ROI using the individual IS model matrix and Desikan-Killiany parcellation (45). To increase trials number, we split epochs into 2 × 0.25-second segments (12,47) of the first 0.5 second after 0.25 second from the stimulus onset (from 0.25 to 0.75 seconds). Nonoverlapping ROIs activated by the

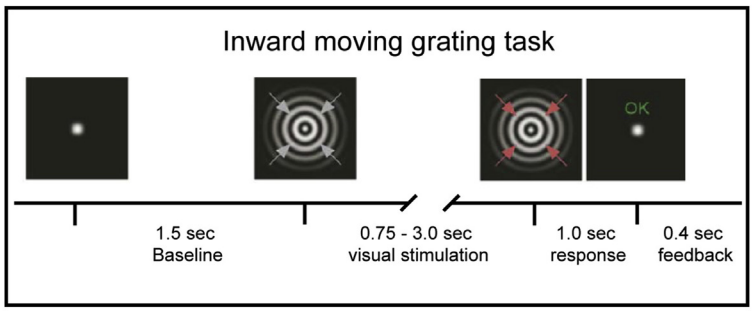

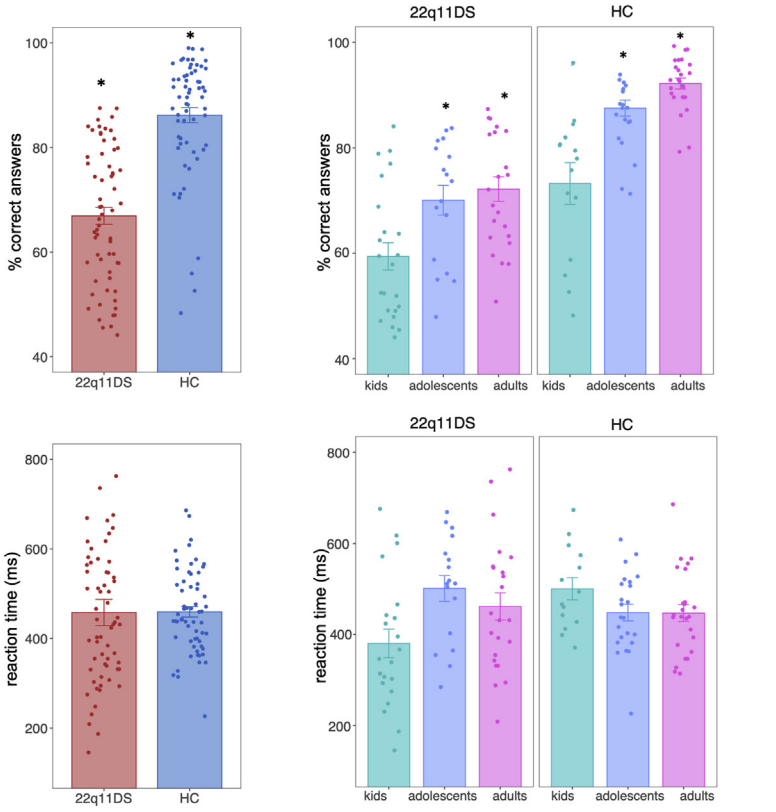

Figure 1. Behavioral results. Upper panel: diagram of the inward-moving grating task. Participants are asked to report the change in speed of inward motion of the grating by button press. Lower panel: bar plots showing group and age subgroup mean and standard deviation for the percentage of correct answers and reaction times (in milliseconds). Asterisks indicate statically significant differences between groups (22q11DS < HC) and subgroups (kids < adolescents, kids < adults). 22q11DS, 22q11.2 deletion syndrome; HC, healthy control.

task belonging to high-order (superior frontal gyrus [SFG]) and low-order areas (cuneus, lateral occipital cortex [LOC]) in the visual system were selected, and GC data from each bilateral pair were averaged over hemisphere. Spectral density matrices were estimated from Fast Fourier–transformed data (0.25–0.75 seconds, 1–80 Hz) with 5-Hz frequency smoothing, matrix factorization, and variance decomposition. Finally, the directionality of connectivity (i.e., feedback vs. feedforward activity) was estimated by computing the direct asymmetry index (12,47).

Statistics

Statistical analyses were performed with MATLAB version 2018a. Independent two-tailed t tests (α level = 0.05) were performed to compare ITPC (from −0.5 to 0.5 seconds), ERSPs (from −0.5 to 0.75 seconds), and GC estimates between control subjects and individuals with 22q11DS.

The age-by-group interaction in behavioral and neurophysiological data was analyzed with two-way analyses of variance with the hierarchical between-subject factors group (control subjects, patients) and age (kids, adolescents, adults), and post hoc analyses were corrected for multiple comparisons using Tukey tests. Multiple linear regression was used to investigate correlations between clinical variables [including behavioral performance, clinical measures, and Full Scale IQ (63)] and neurophysiological data extracted from time-frequency decomposition in deletion carriers. False discovery rate (FDR) correction for multiple comparisons with the Benjamini-Hochberg method (64) was applied to t tests, correcting for the number of frequency bins and time points at

sensor level and, for the number of frequency bins, time points and ROIs at the source level.

FDR correction was also applied for correction of GC between-groups comparison, correcting for the number of frequency bins and couples of nodes tested. FDR-corrected values are reported for the statistically significant time points, indicating the time window and frequency band of significance. Effect sizes were estimated with Cohen's *d*.

RESULTS

Behavioral Data Analysis

A two-way analysis of variance was conducted to examine the effects of group and developmental stage on the percentage of correct responses (Figure 1). There was a significant difference between deletion carriers and healthy control subjects (66% vs. 86%; $F_{1,119} = 73.9$, $p < .001$, partial $\eta^2 = 0.38$) and across age bins ($F_{2,119} = 26.3$, $p < .001$, partial $\eta^2 = 0.30$). However, no age-by-group interaction was detected. Post hoc Tukey tests showed that the performance of children was significantly reduced compared with both adolescents and adults ($p < .001$). No differences were found for average reaction times (457.3 ± 91.2 vs. 460.2 ± 234; $F_{1,119} = 0.02$, $p = .98$, partial $\eta^2 = 0.001$).

ERSP Differences Between Control Subjects and Deletion Carriers

Statistically significant differences between control subjects and deletion carriers were found at gamma- and theta-band frequencies over parieto-occipital electrodes, with deletion carriers having a decreased high and low gamma response during a sustained period (58–68 Hz, 0.25–0.75 seconds, $t_{123} = 3.5$, $p < .001$, $d = 0.98$; 28–44 Hz, $t_{123} = 3$, $p = .0135$, $d = 0.72$) and a decreased early theta response (4–10 Hz, 0–0.4 seconds, $t_{123} = 3.4$, $p < .001$, $d = 0.78$) (Figure 2A). In addition, differences in ITPC were identified in the alpha frequency range (8–14 Hz, 0–0.5 seconds, $t_{123} = 3.8$, $p = .04$) and earlier in beta/

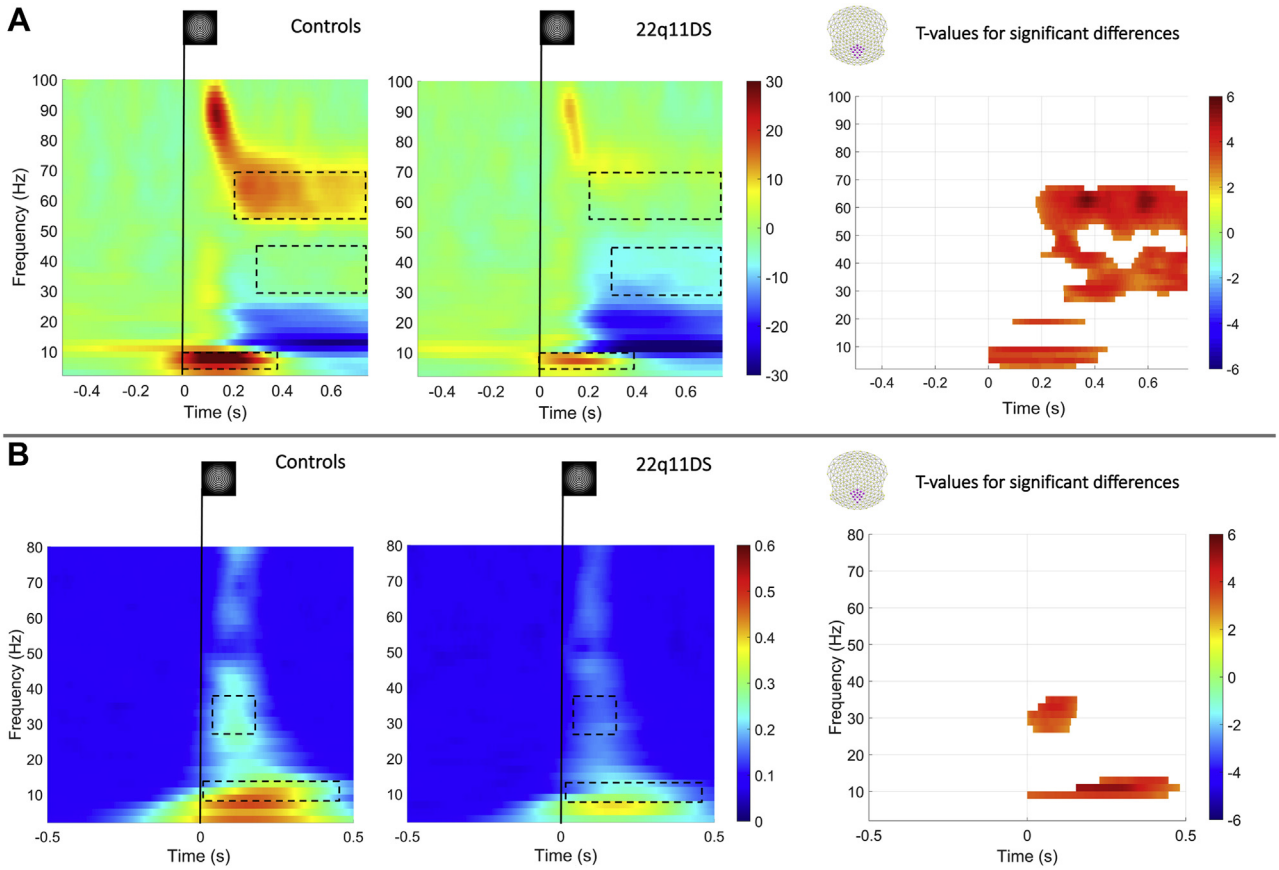

Figure 2. Time-frequency and intertrial phase coherence comparison between control subjects and deletion carriers. **(A)** Time-frequency plots displaying the average pre- and poststimulus event-related spectral perturbation in control subjects and deletion carriers over a cluster of parieto-occipital electrodes. The outlined dotted boxes highlight the time window of statistically significant group differences in high gamma (58–68 Hz), low gamma (28–44 Hz), and theta power (4–10 Hz). On the right side is delta event-related spectral perturbation, showing T values for theta band and high and low gamma band for the cluster of predetermined electrodes. **(B)** Time-frequency plots displaying the average pre- and poststimulus intertrial phase coherence in control subjects and deletion carriers over a cluster of parieto-occipital electrodes. The outlined dotted boxes highlight the time window of statistically significant group differences in alpha (8–14 Hz) and low gamma (26–36 Hz) bands. On the right side is delta intertrial phase coherence showing T values in alpha and low gamma bands for the cluster of predetermined electrodes. Power values are expressed in %. 22q11DS, 22q11.2 deletion syndrome.

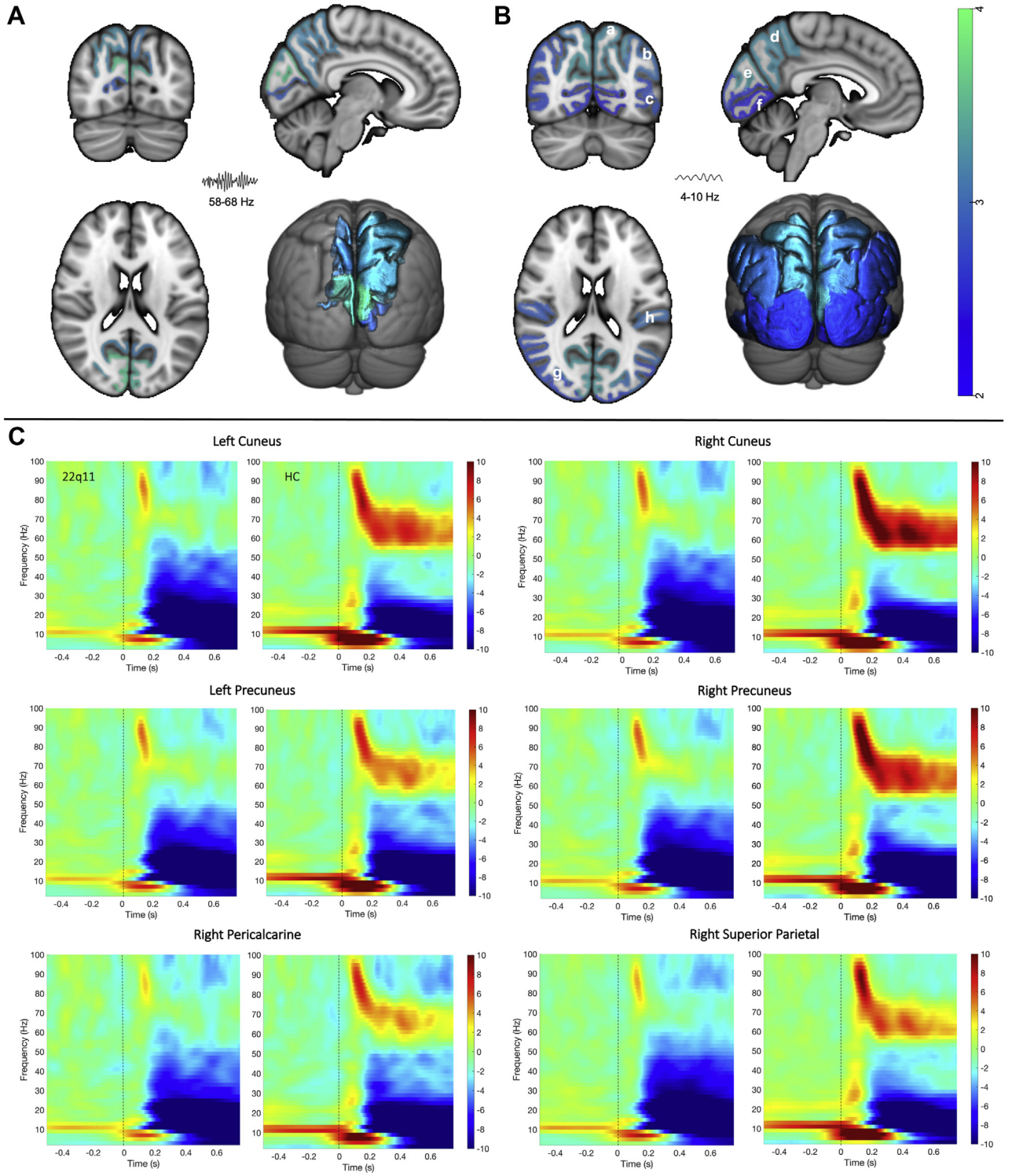

Figure 3. Source space time-frequency analysis between control subjects and deletion carriers. **(A)** Brain map with regions showing a statistically significant decreased gamma response (58–68 Hz, 0–0.75 seconds) in deletion carriers. The colormap represents T values for differences between control subjects and deletion carriers plotted on the brain. **(B)** Brain map with regions showing a statistically significant lower theta response (4–10 Hz, 0–0.5 seconds) in deletion carriers during the first 0.5 second of the response. **(C)** Time-frequency plots for each brain region with decreased gamma response in deletion carriers. The colormap represents power values expressed in %. Regions of interest: a = superior parietal cortex; b = inferior parietal cortex; c = lateral occipital cortex; d = precuneus; e = cuneus; f = lingual gyrus; g = pericalcarine cortex; h = inferior temporal cortex. 22q11DS, 22q11.2 deletion syndrome; HC, healthy control.

low gamma range (26–36 Hz, 0–0.2 seconds, $t_{123} = 3.5$, $p = .006$) (Figure 2B).

Source space analysis revealed a decreased high gamma-band response (58–68 Hz) in deletion carriers in the bilateral cuneus and precuneus and right pericalcarine and superior parietal cortices (Figure 3A, C). In contrast, lower theta (4–8 Hz) responses in deletion carriers were localized to a wider occipital-temporo-parietal network, comprising the bilateral cuneus, pericalcarine cortex, LOC, lingual gyrus, precuneus, superior and inferior parietal cortices, and inferior temporal cortex (Figure 2B).

Between-Groups Differences in Age-Related Gamma, Alpha/Beta, and Theta Responses

To test the age-by-group interaction, we conducted a two-way analysis of variance for each frequency band of interest (i.e., theta, alpha/beta, and gamma) (46,47). We found a statistically significant effect of group ($F_{1,119} = 21.5$, $p < .001$, partial $\eta^2 = 0.16$) and age ($F_{2,119} = 5.3$, $p = .007$, partial $\eta^2 = 0.09$) on gamma-band responses (58–68 Hz, 0.25–0.75 s), with an age-by-group interaction ($F_{2,119} = 3.2$, $p = .04$, partial $\eta^2 = 0.6$). Post hoc analyses with Tukey test(s) showed that gamma-band response in control subjects was significantly higher in adults than in children ($p = .005$) and adolescents ($p = .02$).

There was also a significant effect of group ($F_{1,119} = 5.2$, $p = .025$, partial $\eta^2 = 0.06$) and age ($F_{2,119} = 8.6$, $p < .001$, partial $\eta^2 = 0.15$) on alpha/beta-band desynchronization (10–25 Hz, 0.25–0.75 seconds), without an age-by-group interaction. Post hoc analyses showed that alpha/beta desynchronization in both groups was significantly higher in adults than in children ($p < .001$) and adolescents ($p = .012$) in both groups. Finally, we found a statistically significant effect of group ($F_{1,119} = 22.8$, $p < .001$, partial $\eta^2 = 0.19$) and age ($F_{2,119} = 8.9$, $p < .001$,

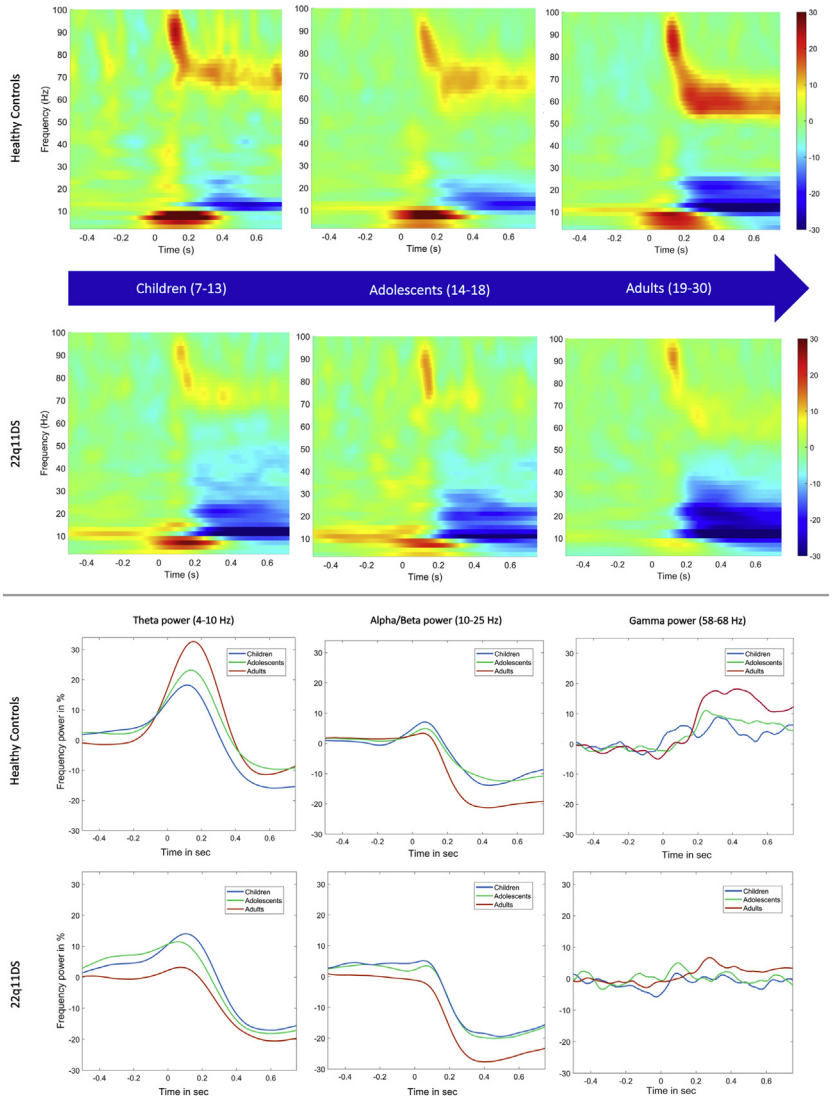

Figure 4. Developmental patterns of oscillatory response. Upper panel: time-frequency plots are shown for each age bin (childhood, adolescence, and adulthood) in the two groups compared: control subjects (above the arrow) and deletion carriers (below the arrow). Statistically significant differences were found only between adult subgroups and between the adult control group vs. the children and adolescent control groups. Lower panel: age subgroups comparison between control subjects and deletion carriers for averaged theta (4–10 Hz), alpha/beta (10–25 Hz), and gamma power (58–68 Hz) over a parieto-occipital cluster of electrodes. Power values are expressed in %. 22q11DS, 22q11.2 deletion syndrome.

partial η^2 = 0.16) on theta-band responses (4–8 Hz, 0–0.5 seconds), with an age-by-group interaction ($F_{2,119}$ = 3.2, p = .04, partial η^2 = 0.09). Post hoc analyses showed that in addition to the higher theta-band response in control subjects compared with deletion carriers, the theta-band response in control subjects was significantly higher in children than in adults (p = .003) and adolescents (p = .011) (Figure 4). To verify whether the lack of statistically significant interaction with age for gamma-band response (58–68 Hz, 0.25–0.75 seconds) in deletion carriers depended on a relatively low sample size, we performed power analyses. With α = 0.05 and power = 0.80, the projected sample size needed is approximately n = 388 for the comparison between adults and adolescents and n = 1000 for the comparison between adults and children. Given the magnitude of the projected sample size to find differences between age subgroups, we concluded that the age-by-group interaction observed reflected blunted developmental trajectories in deletion carriers.

Correlation With Behavioral Performance and Full Scale IQ

We fitted a regression model to test the association between behavioral performance and averaged oscillatory response in high gamma (58–68 Hz), low gamma (28–44 Hz), theta (4–8 Hz), and alpha/beta (10–25 Hz) bands in deletion carriers and control subjects. While the overall regression was not statistically significant for either of the groups, we found that alpha/beta-band response (0.25–0.75 seconds) significantly predicted the number of correct responses (β = −0.54, p = .028) in deletion carriers. In addition, another regression model was fitted to test the association between Full Scale IQ and the neurophysiological data described above, but the overall regression was not statistically significant, and there was no significant interaction with any variable in any group.

GC Connectivity

We found decreased top-down connectivity from the SFG to the LOC at beta frequency (22–40 Hz, t_{123} = −3.18, p = .004, d = −0.7) in control subjects (Figure 5). In addition, control subjects also had increased bottom-up connectivity from the cuneus to the LOC (65–75 Hz, t_{123} = 3.38, p = .004, d = 0.65) and decreased LOC to cuneus connectivity (23–40 Hz, t_{123} = −3.35, p = .015, d = −0.8) as compared with deletion carriers. The directed asymmetry indices were negative for SFG to LOC and for LOC to cuneus connectivity and positive for cuneus to LOC connectivity, indicating feedback and feedforward flow of information between the nodes,

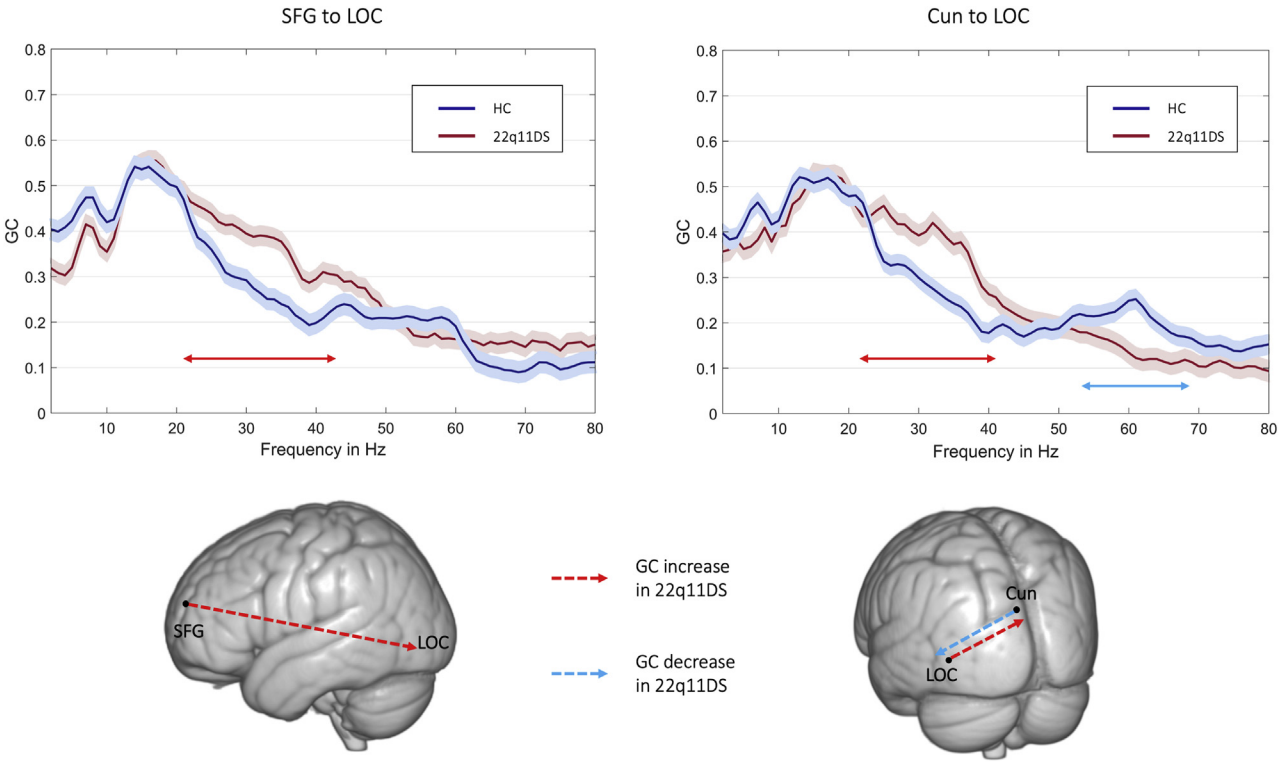

Figure 5. Between-groups GC connectivity differences. Results of the comparison between deletion carriers and control subjects of GC connectivity estimates computed between 0.25 and 0.75 seconds after stimulus. GC values for each group are plotted across the frequency spectrum with error bars indicating SEM, and an arrow indicating the frequency range of significant group effects. The directed asymmetry indices were negative for SFG to LOC and for LOC to Cun connectivity and positive for Cun to LOC connectivity, indicating feedback and feedforward flow of information between the nodes, respectively. On the bottom of the figure, increased (red) and decreased (light blue) GC connections in deletion carriers are plotted on the surface of a standard Montreal Neurological Institute brain in sagittal and coronal planes. 22q11DS, 22q11.2 deletion syndrome; Cun, cuneus; GC, Granger causality; HC, healthy control; LOC, lateral occipital cortex; SFG, superior frontal gyrus.

respectively. No between-groups differences were found for SFG to cuneus GC connectivity.

Psychotic Symptoms and Brain Oscillations

Deletion carriers with APSs (n = 12) were compared with a group of age-matched nonpsychotic individuals with 22q11DS (n = 28). At sensor level, there was a significant reduction in high gamma-band responses (58–68 Hz) in deletion carriers with APS as compared with nonpsychotic deletion carriers, which, however, did not survive FDR correction (Figure S1). We performed a power analysis based on these results and with α = 0.05 and power = 0.80, the projected sample size needed to find a difference in gamma-band response (58–68 Hz, 0.25–0.75 seconds) between the two groups is approximately n = 64.

A regression model was fitted to test the association between Structured Interview for Psychosis-Risk Syndromes positive and negative subscales and averaged gamma-, theta-, or beta-band ERSPs or averaged alpha/beta ITPC amplitude in deletion carriers. The overall regression was not statistically significant, and there was no significant interaction with any variable.

DISCUSSION

In this study, we showed decreased theta- and gamma-band responses to visual stimuli in deletion carriers, together with an increase in top-down connectivity mediated by frontal cortices. In addition, while the maturational patterns of gamma- and theta-band responses were disrupted in individuals with 22q11DS, the development of alpha/beta responses was preserved. Together, these findings provide novel evidence for the involvement of neural oscillations in visual circuit dysfunctions in 22q11DS.

Impaired Theta- and Gamma-Band Responses to Visual Stimuli and Behavioral Correlates

The main finding was a marked decrease in the stimulus-induced power of low/high gamma- and theta-band responses in deletion carriers while alpha/beta desynchronization was intact. Source analysis localized group differences to occipital-parietal regions. The recruitment of these regions is consistent with previous studies (7,12,47). In contrast, decreased theta/gamma-band activity in visual areas in deletion carriers highlights the involvement of aberrant circuitry in sensory areas in 22q11DS. Compromised local circuit activity in V1 with decreased stimulus-elicited gamma- and theta-band responses has been similarly identified in the homologous mice model of 22q11DS (38). Several genes within the 22q11.2 region are implicated in interneuron migration (41,42) and GABAergic and glutamatergic signaling (39). Given the involvement of GABAergic and glutamatergic neural transmission in the generation of gamma-band oscillations (15), it is possible that the gamma-band response impairment identified in mice and human deletion carriers may be associated with the haploinsufficiency of key genes.

In contrast to the impairment in gamma-band responses, alpha/beta desynchronization was spared in individuals with 22q11DS. Furthermore, the subgroup of adult deletion carriers displayed even enhanced desynchronization compared with control subjects, which correlated with performance levels. Gamma and alpha/beta oscillations have been proposed to subserve distinct roles in information processing as well as involve different neural substrates. While gamma oscillations reflect the feedforward propagation of sensory stimuli (50,65), alpha and beta oscillations mediate top-down information representing the attention allocation toward visual stimuli (66–68). Moreover, the generation of distinct rhythms is also associated with different cortical layers (65,69). Gamma oscillations are assumed to arise from supragranular layers, while alpha/beta oscillations arise from infragranular layers. Studies in a mouse model of 22q11DS highlighted a disruption in the proliferation of basal progenitors, which predominantly give rise to supragranular pyramidal cells later in life (40), and altered migration of interneurons (41,42). Thus, the dissociation between impaired theta/gamma and preserved alpha/beta-band responses identified in our data may reflect a selective impairment of supragranular projection neurons and interneuron dysfunction in individuals with 22q11DS. Future research is needed to test this hypothesis.

Increased Alpha/Beta Desynchronization and Top-Down Connectivity in Deletion Carriers

We further explored frequency-resolved directed connectivity between high- and low-order visual areas and observed enhanced feedback information flow from the prefrontal cortex to the LOC at beta frequencies, while the feedforward communication in higher frequencies from V1 to LOC was impaired in deletion carriers. In normal conditions, heightened top-down control exerted over visual areas leads to increased gamma-band power (70,71), thus modulating sensory processing according to the behavioral context (72). However, despite increased top-down modulation of lower-order areas, deletion carriers display profound impairment in gamma-band response in the primary visual cortex and decreased bottom-up gamma signaling between primary and secondary visual areas.

Increased top-down and decreased bottom-up connectivity has been also identified in patients at clinical high risk for psychosis and patients with first episode of psychosis (12), suggesting a close overlap between circuit deficits caused by 22q11.2 deletion and early-stage psychosis. Moreover, previous ERSP studies in 22q11DS found enhanced feedback activity (36) and increased amplitude in negative late-latency components localized to the frontal cortex (37). Overall, elevated top-down modulation of visual areas in this study may constitute a compensatory mechanism for impaired feedforward activity in early sensory regions.

Differential Impact of Age on Frequency Bands

Our final aim was to investigate how neural oscillations during visual perception change during brain development. In control subjects, we identified age-related changes in induced power for theta-band (4–8 Hz), alpha/beta-band (10–25 Hz), and high gamma-band (58–68 Hz) oscillations during adolescence, which are consistent with previous findings (24). Remarkably, while deletion carriers exhibited preserved developmental patterns for alpha/beta frequencies, the age-related increase in gamma-band responses was largely absent.

Adolescence is characterized by the protracted maturation of both GABAergic neural transmission (73), including parvalbumin interneurons (20), and NMDA receptor expression (23) that could underlie the late development of high-frequency oscillations (18,19). Accordingly, it is conceivable that the failure to express adult-level gamma-band responses in deletion carriers is related to aberrant maturation of GABAergic and glutamatergic circuit motifs that could potentially also contribute to the risk of developing psychosis in 22q11 deletion carriers.

These findings are in line with previous studies showing reduced gamma-band response to auditory stimuli in deletion carriers and a similar developmental profile (45). In both deletion carriers and patients with idiopathic psychotic disorders, decreased gamma-band responses to auditory stimuli have been identified predominantly in the temporal cortex (2,44,45,74). Likewise, gamma oscillation impairment during visual processing has been mapped to the occipital cortex (7,12). Studies using magnetic resonance spectroscopy (MRS) and positron emission tomography imaging have demonstrated a correlation between gamma-band power during auditory and visual tasks and GABA (gamma-aminobutyric acid) concentration or $GABA_A$ receptor density, respectively (75,76). Thus, findings of gamma-band impairment are in agreement with postmortem and MRS studies in patients with schizophrenia showing a marked reduction of GABA concentration in occipital and auditory cortices (77–80).

An interesting perspective is that the identified deficits in gamma-band response to sensory stimuli may be related to the disruption of GABAergic signaling also in 22q11DS. Studies conducted so far in 22q11DS to examine GABA are conflicting, with a lack of human MRS evidence for altered GABA concentration in the anterior cingulate cortex (81) but findings of abnormal GABA release and response to $GABA_A$ receptor antagonists in mice models (82). Such discrepancies could be explained by inherent limitations of the MRS technique to distinguish between intra- and extracellular compartments (83) and the choice of the explored region. Future studies are required to assess GABA concentration in brain regions implicated in sensory processing and to link it to gamma-band response in 22q11DS.

Limitations

First, these data are based on cross-sectional findings. Second, despite previous research showing an increasing reduction of gamma-band response throughout the progression of psychosis (12), no statistically significant differences in ERSP or ITPC were found between deletion carriers with and without APSs. Our exploratory analysis highlighted that the sample size for this subanalysis was slightly underpowered. Thus, we can hypothesize that given the relevance of deficits of visuospatial perception in all the subjects with a 22q11.2 microdeletion, a further decline in gamma-band response to visual stimuli in subjects endorsing psychotic symptoms may be harder to capture with relatively small sample sizes. Future studies with an adequate sample size are required to further explore differences in gamma-band response to visual stimuli between deletion carriers with and without APSs.

Conclusions

This study offers novel insight into the neurobiology of visual circuit deficits in individuals with 22q11DS. Specifically, our findings suggest that impairments in gamma-band responses may lead to decreased bottom-up signaling, which in turn is associated with enhanced recruitment of top-down attentional control. Our data, by highlighting the importance of early intervention to improve developmental trajectories during critical phases of brain development, could potentially inform novel treatment strategies that target circuit deficits underlying visual impairments and the associated neurobiological mechanisms in deletion carriers.

ACKNOWLEDGMENTS AND DISCLOSURES

This work was supported by research grants from the Swiss National Science Foundation (Grant Nos. 324730_144260 and 320030-179404 [to SE] and Grant No. 320030_184677 [to CMM]) and a National Centre of Competence in Research Synapsy grant (Grant No. 51NF40-185897 [to SE and CMM]). This study was also supported by the Human Neuroscience Platform, Fondation Campus Biotech Geneva, Geneva, Switzerland.

We thank all the families who contributed to the study as well as the family associations (Generation 22, Connect 22, and Relais 22) for their ongoing support. We particularly thank the managers and operators of the EEG and MRI platforms Gwenaël Birot, Roberto Martuzzi and Loan Mattera. Special thanks go to Virginie Pouillard, Eva Micol and Tereza Kotalova for coordinating the project, to Lucia Cantonas, Johanna Maeder, Joëlle Bagautdinova, Lydia Dubourg, Farnaz Delavari and Karin Bortolin for their help in the acquisition of the data and to Hanna Thuné for her help with the EEG paradigm implementation.

The authors report no biomedical financial interests or potential conflicts of interest.

ARTICLE INFORMATION

From the Developmental Imaging and Psychopathology Laboratory (VM, CL, SE) and Department of Genetic Medicine and Development (SE), University of Geneva School of Medicine; Functional Brain Mapping Laboratory (VR, MS, TAR, CMM), Department of Basic Neurosciences, University of Geneva; Human Neuroscience Platform (VR), Fondation Campus Biotech Geneva, Geneva; Center for Biomedical Imaging (CMM), Lausanne, Switzerland; Institute of Neuroscience and Psychology (TG, PJU), University of Glasgow, Glasgow, Scotland; and the Department of Child and Adolescent Psychiatry, Psychosomatic Medicine and Psychotherapy (TG, PJU), Charité Universitätsmedizin, Berlin, Germany.

CMM and SE contributed equally to this work as supervisors.

Address correspondence to Valentina Mancini, M.D., at valentina.mancini@unige.ch.

Received Dec 10, 2021; revised Feb 24, 2022; accepted Feb 25, 2022.

Supplementary material cited in this article is available online at https://doi.org/10.1016/j.biopsych.2022.02.961.

REFERENCES

1. Spencer KM (2008): Visual gamma oscillations in schizophrenia: Implications for understanding neural circuitry abnormalities. Clin EEG Neurosci 39:65–68.
2. Reilly TJ, Nottage JF, Studerus E, Rutigliano G, De Micheli AI, Fusar-Poli P, McGuire P (2018): Gamma band oscillations in the early phase of psychosis: A systematic review. Neurosci Biobehav Rev 90:381–399.
3. Gandal MJ, Edgar JC, Klook K, Siegel SJ (2012): Gamma synchrony: Towards a translational biomarker for the treatment-resistant symptoms of schizophrenia. Neuropharmacology 62:1504–1518.
4. Tada M, Nagai T, Kirihara K, Koike S, Suga M, Araki T, *et al.* (2016): Differential alterations of auditory gamma oscillatory responses

between pre-onset high-risk individuals and first-episode schizophrenia. Cereb Cortex 26:1027–1035.
5. Tan HRM, Lana L, Uhlhaas PJ (2013): High-frequency neural oscillations and visual processing deficits in schizophrenia. Front Psychol 4:621.
6. Grützner C, Wibral M, Sun L, Rivolta D, Singer W, Maurer K, Uhlhaas PJ (2013): Deficits in high- (>60 Hz) gamma-band oscillations during visual processing in schizophrenia. Front Hum Neurosci 7:88.
7. Shaw AD, Knight L, Freeman TCA, Williams GM, Moran RJ, Friston KJ, *et al.* (2020): Oscillatory, computational, and behavioral evidence for impaired GABAergic inhibition in schizophrenia. Schizophr Bull 46:345–353.
8. Riečanský I, Kašpárek T, Řehulová J, Katina S, Přikryl R (2010): Aberrant EEG responses to gamma-frequency visual stimulation in schizophrenia. Schizophr Res 124:101–109.
9. Spencer KM, Nestor PG, Perlmutter R, Niznikiewicz MA, Klump MC, Frumin M, *et al.* (2004): Neural synchrony indexes disordered perception and cognition in schizophrenia. Proc Natl Acad Sci U S A 101:17288–17293.
10. Sauer A, Grent-'t-Jong T, Wibral M, Grube M, Singer W, Uhlhaas PJ (2020): A MEG study of visual repetition priming in schizophrenia: Evidence for impaired high-frequency oscillations and event-related fields in thalamo-occipital cortices. Front Psychiatry 11:561973.
11. Javitt DC (2009): Sensory processing in schizophrenia: Neither simple nor intact. Schizophr Bull 35:1059–1064.
12. Grent-'t-Jong T, Gajwani R, Gross J, Gumley AI, Krishnadas R, Lawrie SM, *et al.* (2020): Association of magnetoencephalographically measured high-frequency oscillations in visual cortex with circuit dysfunctions in local and large-scale networks during emerging psychosis [published correction appears in JAMA Psychiatry 2020; 77: 652]. JAMA Psychiatry 77:852–862.
13. Markram H, Toledo-Rodriguez M, Wang Y, Gupta A, Silberberg G, Wu C (2004): Interneurons of the neocortical inhibitory system. Nat Rev Neurosci 5:793–807.
14. Börgers C, Epstein S, Kopell NJ (2005): Background gamma rhythmicity and attention in cortical local circuits: A computational study. Proc Natl Acad Sci U S A 102:7002–7007.
15. Cardin JA, Carlén M, Meletis K, Knoblich U, Zhang F, Deisseroth K, *et al.* (2009): Driving fast-spiking cells induces gamma rhythm and controls sensory responses. Nature 459:663–667.
16. Fries P, Nikolić D, Singer W (2007): The gamma cycle. Trends Neurosci 30:309–316.
17. Buzśaki G, Wang XJ (2012): Mechanisms of gamma oscillations. Annu Rev Neurosci 35:203–225.
18. Uhlhaas PJ, Singer W (2011): The development of neural synchrony and large-scale cortical networks during adolescence: Relevance for the pathophysiology of schizophrenia and neurodevelopmental hypothesis. Schizophr Bull 37:514–523.
19. Uhlhaas PJ, Roux F, Rodriguez E, Rotarska-Jagiela A, Singer W (2010): Neural synchrony and the development of cortical networks. Trends Cogn Sci 14:72–80.
20. Morishita H, Kundakovic M, Bicks L, Mitchell A, Akbarian S (2015): Interneuron epigenomes during the critical period of cortical plasticity: Implications for schizophrenia. Neurobiol Learn Mem 124:104–110.
21. Hoftman GD, Lewis DA (2011): Postnatal developmental trajectories of neural circuits in the primate prefrontal cortex: Identifying sensitive periods for vulnerability to schizophrenia. Schizophr Bull 37:493–503.
22. Pafundo DE, Pretell Annan CA, Fulginiti NM, Belforte JE (2021): Early NMDA receptor ablation in interneurons causes an activity-dependent E/I imbalance in vivo in prefrontal cortex pyramidal neurons of a mouse model useful for the study of schizophrenia. Schizophr Bull 47:1300–1309.
23. Wang HX, Gao WJ (2009): Cell type-specific development of NMDA receptors in the interneurons of rat prefrontal cortex. Neuropsychopharmacology 34:2028–2040.
24. Uhlhaas PJ, Roux F, Singer W, Haenschel C, Sireteanu R, Rodriguez E (2009): The development of neural synchrony reflects late maturation and restructuring of functional networks in humans. Proc Natl Acad Sci U S A 106:9866–9871.
25. Mukherjee A, Carvalho F, Eliez S, Caroni P, *et al.* (2019): Long-lasting rescue of network and cognitive dysfunction in a genetic schizophrenia model. Cell 178:1387–1402.e14.
26. Monks S, Niarchou M, Davies AR, Walters JTR, Williams N, Owen MJ, *et al.* (2014): Further evidence for high rates of schizophrenia in 22q11.2 deletion syndrome. Schizophr Res 153:231–236.
27. Schneider M, Debbané M, Bassett AS, Chow EWC, Fung WLA, Van Den Bree M, *et al.* (2014): Psychiatric disorders from childhood to adulthood in 22q11.2 deletion syndrome: Results from the International Consortium on Brain and Behavior in 22q11.2 Deletion Syndrome. Am J Psychiatry 171:627–639.
28. Tang SX, Moore TM, Calkins ME, Yi JJ, Savitt A, Kohler CG, *et al.* (2017): The psychosis spectrum in 22q11.2 deletion syndrome is comparable to that of nondeleted youths. Biol Psychiatry 82:17–25.
29. Zinkstok JR, Boot E, Bassett AS, Hiroi N, Butcher NJ, Vingerhoets C, *et al.* (2019): Neurobiological perspective of 22q11.2 deletion syndrome. Lancet Psychiatry 6:951–960.
30. Sun D, Ching CRK, Lin A, Forsyth JK, Kushan L, Vajdi A, *et al.* (2020): Large-scale mapping of cortical alterations in 22q11.2 deletion syndrome: Convergence with idiopathic psychosis and effects of deletion size. Mol Psychiatry 25:1822–1834.
31. Cleynen I, Engchuan W, Hestand MS, Heung T, Holleman AM, Johnston HR, *et al.* (2021): Genetic contributors to risk of schizophrenia in the presence of a 22q11.2 deletion. Mol Psychiatry 26:4496–4510.
32. Bearden CE, Woodin MF, Wang PP, Moss E, McDonald-McGinn D, Zackai E, *et al.* (2001): The neurocognitive phenotype of the 22q11.2 deletion syndrome: Selective deficit in visual-spatial memory. J Clin Exp Neuropsychol 23:447–464.
33. McCabe KL, Marlin S, Cooper G, Morris R, Schall U, Murphy DG, *et al.* (2016): Visual perception and processing in children with 22q11.2 deletion syndrome: Associations with social cognition measures of face identity and emotion recognition. J Neurodev Disord 8:30.
34. Mccabe KL, Popa AM, Durdle C, Amato M, Cabaral MH, Cruz J, *et al.* (2019): Quantifying the resolution of spatial and temporal representation in children with 22q11.2 deletion syndrome. J Neurodev Disord 11:40.
35. Bostelmann M, Schneider M, Padula MC, Maeder J, Schaer M, Scariati E, *et al.* (2016): Visual memory profile in 22q11.2 microdeletion syndrome: Are there differences in performance and neurobiological substrates between tasks linked to ventral and dorsal visual brain structures? A cross-sectional and longitudinal study. J Neurodev Disord 8:41.
36. Magnée MJCM, Lamme VAF, de Sain-van der Velden MGM, Vorstman JAS, Kemner C (2011): Proline and COMT Status affect visual connectivity in children with 22q11.2 deletion syndrome. PLoS One 6:e25882.
37. Biria M, Tomescu MI, Custo A, Cantonas LM, Song KW, Schneider M, *et al.* (2017): Visual processing deficits in 22q11.2 deletion syndrome. Neuroimage Clin 17:976–986.
38. Hamm JP, Peterka DS, Gogos JA, Yuste R (2017): Altered cortical ensembles in mouse models of schizophrenia. Neuron 94:153–167.e8.
39. Motahari Z, Moody SA, Maynard TM, Lamantia AS (2019): In the line-up: Deleted genes associated with DiGeorge/22q11.2 deletion syndrome: Are they all suspects? J Neurodev Disord 11:7.
40. Meechan DW, Tucker ES, Maynard TM, LaMantia AS (2009): Diminished dosage of 22q11 genes disrupts neurogenesis and cortical development in a mouse model of 22q11 deletion/DiGeorge syndrome. Proc Natl Acad Sci U S A 106:16434–16445.
41. Meechan DW, Tucker ES, Maynard TM, LaMantia AS (2012): Cxcr4 regulation of interneuron migration is disrupted in 22q11.2 deletion syndrome. Proc Natl Acad Sci U S A 109:18601–18606.
42. Toritsuka M, Kimoto S, Muraki K, Landek-Salgado MA, Yoshida A, Yamamoto N, *et al.* (2013): Deficits in microRNA-mediated Cxcr4/Cxcl12 signaling in neurodevelopmental deficits in a 22q11 deletion syndrome mouse model. Proc Natl Acad Sci U S A 110:17552–17557.

43. Pocklington AJ, Rees E, Walters JTR, Han J, Kavanagh DH, Chambert KD, *et al.* (2015): Novel findings from CNVs implicate inhibitory and excitatory signaling complexes in schizophrenia. Neuron 86:1203–1214.
44. Larsen KM, Pellegrino G, Birknow MR, Kjær TN, Baaré WFC, Didriksen M, *et al.* (2018): 22q11.2 deletion syndrome is associated with impaired auditory steady-state gamma response. Schizophr Bull 44:388–397.
45. Mancini V, Rochas V, Seeber M, Roehri N, Rihs TA, Ferat V, *et al.* (2022): Aberrant developmental patterns of gamma-band response and long-range communication disruption in youths with 22q11.2 deletion syndrome. Am J Psychiatry 179:204–215.
46. Bastos AM, Vezoli J, Bosman CA, Schoffelen JM, Oostenveld R, Dowdall JR, *et al.* (2015): Visual areas exert feedforward and feedback influences through distinct frequency channels. Neuron 85:390–401.
47. Michalareas G, Vezoli J, van Pelt S, Schoffelen JM, Kennedy H, Fries P (2016): Alpha-beta and gamma rhythms subserve feedback and feedforward influences among human visual cortical areas. Neuron 89:384–397.
48. Buffalo EA, Fries P, Landman R, Buschman TJ, Desimone R (2011): Laminar differences in gamma and alpha coherence in the ventral stream. Proc Natl Acad Sci U S A 108:11262–11267.
49. Miller TJ, McGlashan TH, Rosen JL, Cadenhead K, Cannon T, Ventura J, *et al.* (2003): Prodromal assessment with the structured interview for prodromal syndromes and the scale of prodromal symptoms: Predictive validity, interrater reliability, and training to reliability [published correction appears in Schizophr Bull 2004; 30: following 217]. Schizophr Bull 29:703–715.
50. Hoogenboom N, Schoffelen JM, Oostenveld R, Parkes LM, Fries P (2006): Localizing human visual gamma-band activity in frequency, time and space. Neuroimage 29:764–773.
51. Makeig S, Jung TP, Bell AJ, Ghahremani D, Sejnowski TJ (1997): Blind separation of auditory event-related brain responses into independent components. Proc Natl Acad Sci U S A 94:10979–10984.
52. Jung TP, Makeig S, Westerfield M, Townsend J, Courchesne E, Sejnowski TJ (2000): Removal of eye activity artifacts from visual event-related potentials in normal and clinical subjects. Clin Neurophysiol 111:1745–1758.
53. Perrin F, Pernier J, Bertrand O, Echallier JF (1989): Spherical splines for scalp potential and current density mapping. Electroencephalogr Clin Neurophysiol 72:184–187.
54. Cantonas LM, Mancini V, Rihs TA, Rochas V, Schneider M, Eliez S, Michel CM (2021): Abnormal auditory processing and underlying structural changes in 22q11.2 deletion syndrome. Schizophr Bull 47:189–196.
55. Neuper C, Pfurtscheller G (2001): Event-related dynamics of cortical rhythms: Frequency-specific features and functional correlates. Int J Psychophysiol 43:41–58.
56. Delorme A, Makeig S (2004): EEGLAB: An open source toolbox for analysis of single-trial EEG dynamics including independent component analysis. J Neurosci Methods 134:9–21.
57. Fischl B (2012). FreeSurfer. Neuroimage 62:774–781.
58. Michel CM, Brunet D (2019): EEG source imaging: A practical review of the analysis steps. Front Neurol 10:325.
59. Brunet D, Murray MM, Michel CM (2011): Spatiotemporal analysis of multichannel EEG: CARTOOL. Comput Intell Neurosci 2011:813870.
60. Desikan RS, Ségonne F, Fischl B, Quinn BT, Dickerson BC, Blacker D, *et al.* (2006): An automated labeling system for subdividing the human cerebral cortex on MRI scans into gyral based regions of interest. Neuroimage 31:968–980.
61. Dhamala M, Rangarajan G, Ding M (2008): Analyzing information flow in brain networks with nonparametric Granger causality. Neuroimage 41:354–362.
62. Oostenveld R, Fries P, Maris E, Schoffelen JM (2011): FieldTrip: Open source software for advanced analysis of MEG, EEG, and invasive electrophysiological data. Comput Intell Neurosci 2011:156869.
63. Weschler D (2011): WAIS-IV: Administration and Scoring Manual. San Antonio: Pearson.
64. Benjamini Y, Hochberg Y (1995): Controlling the false discovery rate: A practical and powerful approach to multiple testing. J R Stat Soc B 57:289–300.
65. Fries P (2015): Rhythms for cognition: Communication through coherence. Neuron 88:220–235.
66. Klimesch W (2012): α-band oscillations, attention, and controlled access to stored information. Trends Cogn Sci 16:606–617.
67. Rihs TA, Michel CM, Thut G (2009): A bias for posterior α-band power suppression versus enhancement during shifting versus maintenance of spatial attention. Neuroimage 44:190–199.
68. Romei V, Rihs T, Brodbeck V, Thut G (2008): Resting electroencephalogram alpha-power over posterior sites indexes baseline visual cortex excitability. Neuroreport 19:203–208.
69. Shaw AD, Moran RJ, Muthukumaraswamy SD, Brealy J, Linden DE, Friston KJ, Singh KD (2017): Neurophysiologically-informed markers of individual variability and pharmacological manipulation of human cortical gamma. Neuroimage 161:19–31.
70. Grothe I, Neitzel SD, Mandon S, Kreiter AK (2012): Switching neuronal inputs by differential modulations of gamma-band phase-coherence. J Neurosci 32:16172–16180.
71. Lee JH, Whittington MA, Kopell NJ (2013): Top-down beta rhythms support selective attention via interlaminar interaction: A model. PLoS Comput Biol 9:e1003164.
72. Gilbert CD, Li W (2013): Top-down influences on visual processing. Nat Rev Neurosci 14:350–363.
73. Hashimoto T, Nguyen QL, Rotaru D, Keenan T, Arion D, Beneyto M, *et al.* (2009): Protracted developmental trajectories of GABAA receptor α1 and α2 subunit expression in primate prefrontal cortex. Biol Psychiatry 65:1015–1023.
74. Thuné H, Recasens M, Uhlhaas PJ (2016): The 40-Hz auditory steady-state response in patients with schizophrenia: A meta-analysis. JAMA Psychiatry 73:1145–1153.
75. Kujala J, Jung J, Bouvard S, Lecaignard F, Lothe A, Bouet R, *et al.* (2015): Gamma oscillations in V1 are correlated with GABAA receptor density: A multi-modal MEG and flumazenil-PET study. Sci Rep 5:16347.
76. Balz J, Keil J, Roa Romero Y, Mekle R, Schubert F, Aydin S, *et al.* (2016): GABA concentration in superior temporal sulcus predicts gamma power and perception in the sound-induced flash illusion. Neuroimage 125:724–730.
77. Yoon JH, Maddock RJ, Rokem A, Silver MA, Minzenberg MJ, Ragland JD, Carter CS (2010): GABA concentration is reduced in visual cortex in schizophrenia and correlates with orientation-specific surround suppression. J Neurosci 30:3777–3781.
78. McCutcheon RA, Krystal JH, Howes OD (2020): Dopamine and glutamate in schizophrenia: Biology, symptoms and treatment. World Psychiatry 19:15–33.
79. de Jonge JC, Vinkers CH, Hulshoff Pol HE, Marsman A (2017): GABAergic mechanisms in schizophrenia: Linking postmortem and in vivo studies. Front Psychiatry 8:118.
80. Thakkar KN, Rösler L, Wijnen JP, Boer VO, Klomp DWJ, Cahn W, *et al.* (2017): 7T proton magnetic resonance spectroscopy of gamma-aminobutyric acid, glutamate, and glutamine reveals altered concentrations in patients with schizophrenia and healthy siblings. Biol Psychiatry 81:525–535.
81. Vingerhoets C, Tse DH, van Oudenaren M, Hernaus D, van Duin E, Zinkstok J, *et al.* (2020): Glutamatergic and GABAergic reactivity and cognition in 22q11.2 deletion syndrome and healthy volunteers: A randomized double-blind 7-Tesla pharmacological MRS study. J Psychopharmacol 34:856–863.
82. Kimoto S, Muraki K, Toritsuka M, Mugikura S, Kajiwara K, Kishimoto T, *et al.* (2012): Selective overexpression of Comt in prefrontal cortex rescues schizophrenia-like phenotypes in a mouse model of 22q11 deletion syndrome. Transl Psychiatry 2:e146.
83. Myers JFM, Evans CJ, Kalk NJ, Edden RAE, Lingford-Hughes AR (2014): Measurement of GABA using J-difference edited 1H-MRS following modulation of synaptic GABA concentration with tiagabine. Synapse 68:355–362.